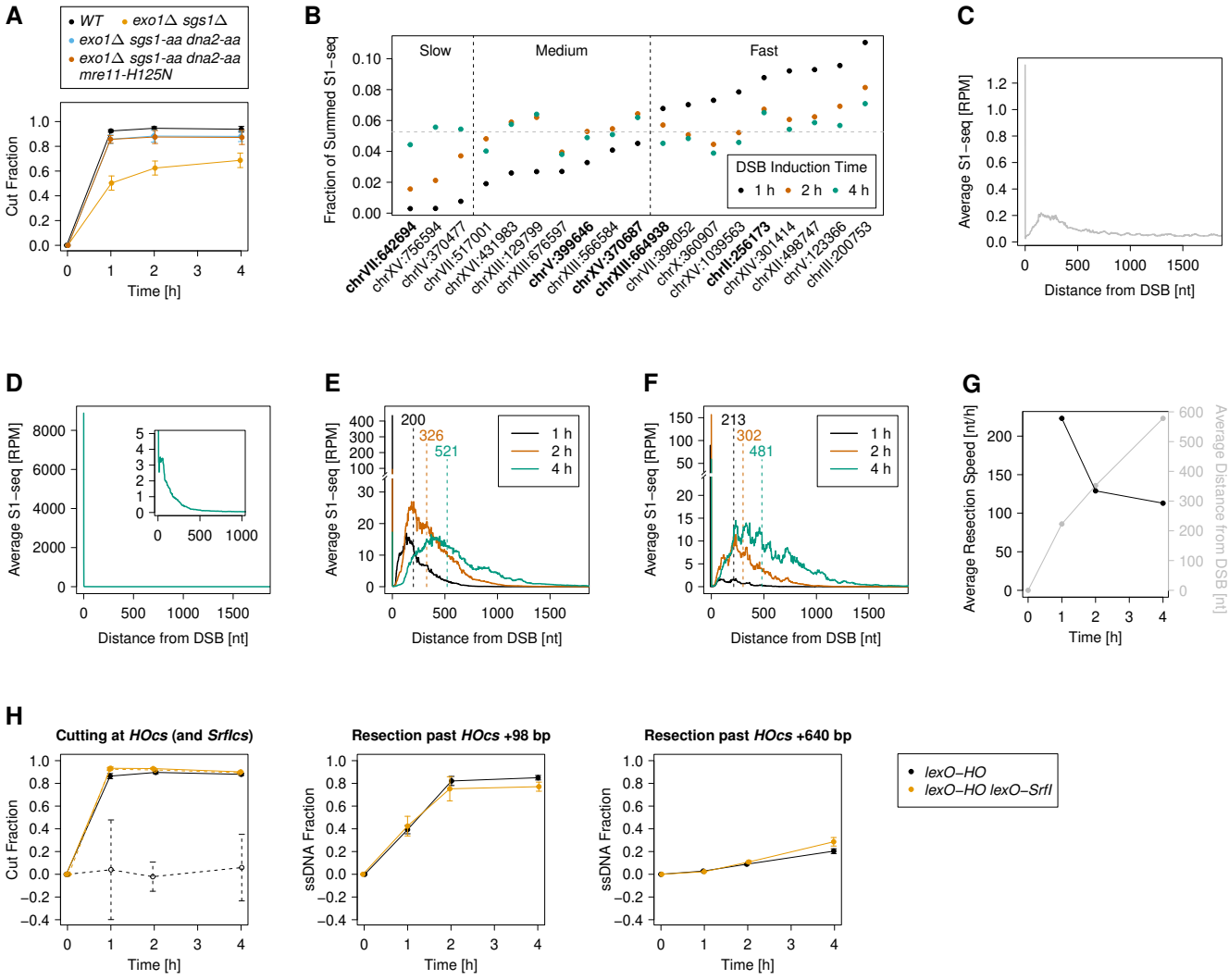
A
WT
exo1Δ sgs1Δ
exo1Δ sgs1-aa dna2-aa
exo1Δ sgs1-aa dna2-aa mre11-H125N
Cut Fraction
Time [h]
B
Slow
Medium
Fast
Fraction of Summed S1−seq
DSB Induction Time
1 h
2 h
4 h
chrVII:642694
chrXV:756594
chrIV:370477
chrVII:517001
chrXVI:431983
chrXIII:129799
chrXIII:676597
chrV:399646
chrXIII:566584
chrXV:370687
chrXIII:664938
chrVII:398052
chrX:360907
chrXV:1039563
chrII:256173
chrXIV:301414
chrXII:498747
chrV:123366
chrIII:200753
C
Average S1−seq [RPM]
Distance from DSB [nt]
D
Average S1−seq [RPM]
Distance from DSB [nt]
E
200
326
521
1 h
2 h
4 h
Average S1−seq [RPM]
Distance from DSB [nt]
F
213
302
481
1 h
2 h
4 h
Average S1−seq [RPM]
Distance from DSB [nt]
G
Average Resection Speed [nt/h]
Average Distance from DSB [nt]
Time [h]
H
Cutting at HOcs (and SrfIcs)
Resection past HOcs +98 bp
Resection past HOcs +640 bp
Cut Fraction
ssDNA Fraction
Time [h]
lexO−HO
lexO−HO lexO−SrfI

Figure S1: Monitoring MRX nicking at nucleotide-resolution, related to Figure 1

(A) DSB formation kinetics related to Figure 1B. DSB formation at *MAT*a *hocs::SrfIcs* was monitored in the indicated strains. Data are represented as mean ± standard deviation (SD) of three biological replicates.

(B) Grouping of DSB formation kinetics into categories "slow", "medium", and "fast". If all DSBs were cut with the same kinetics, the fraction of summed S1-seq coverage around all DSBs would have the same average value (dashed gray horizontal line). Lower and higher values at early time points indicate slow and fast cutting, respectively. DSBs were ordered according to their values at the 1 h time point and manually grouped into kinetic categories. As expected, the values became more equal at later time points, when DSB levels at medium and slowly cut sites had caught up. Genomic coordinates of DSB sites are indicated on the x-axis. Cutting at the DSB sites typeset in bold had been evaluated by qPCR in (Gnügge and Symington, 2020). The ranking of DSB kinetics in this independent assay was the same as shown here, supporting the validity of our approach.

(C) Average 51-nt smoothed S1-seq coverage around the 9 most efficiently formed DSBs prior to SrfI induction.

(D) Average 51-nt smoothed S1-seq coverage around the 9 most efficiently formed DSBs in a long-range resection suppressed *mre11-H125N* strain (4 h after DSB induction). The inset shows a zoom-in with adjusted y-axis for improved visualization of residual resection.

(E and **F)** Average 51-nt smoothed S1-seq coverage spreading from DSBs with medium (E) and slow (F) formation kinetics, as defined in (B). Numbers above vertical dashed lines indicate average spreading distance from DSBs.

(G) Average spreading distance from DSBs (resection tract length) and resection speed over time.

(H) MRX nicking activity is not titrated by multiple DSBs. (Left panel) DSB formation at the *MAT*a HO cut site (*HOcs*) (solid lines) and at the genomic SrfI cut site at chrII:256173 (dashed lines). (Middle and right panel) Resection past the indicated sites. In the *lexO-HO* strain, only a single DSB is formed at *MAT*a *HOcs*, while 20 additional DSBs are formed in the *lexO-HO lexO-SrfI* strain. Data are represented as mean ± SD of three biological replicates.

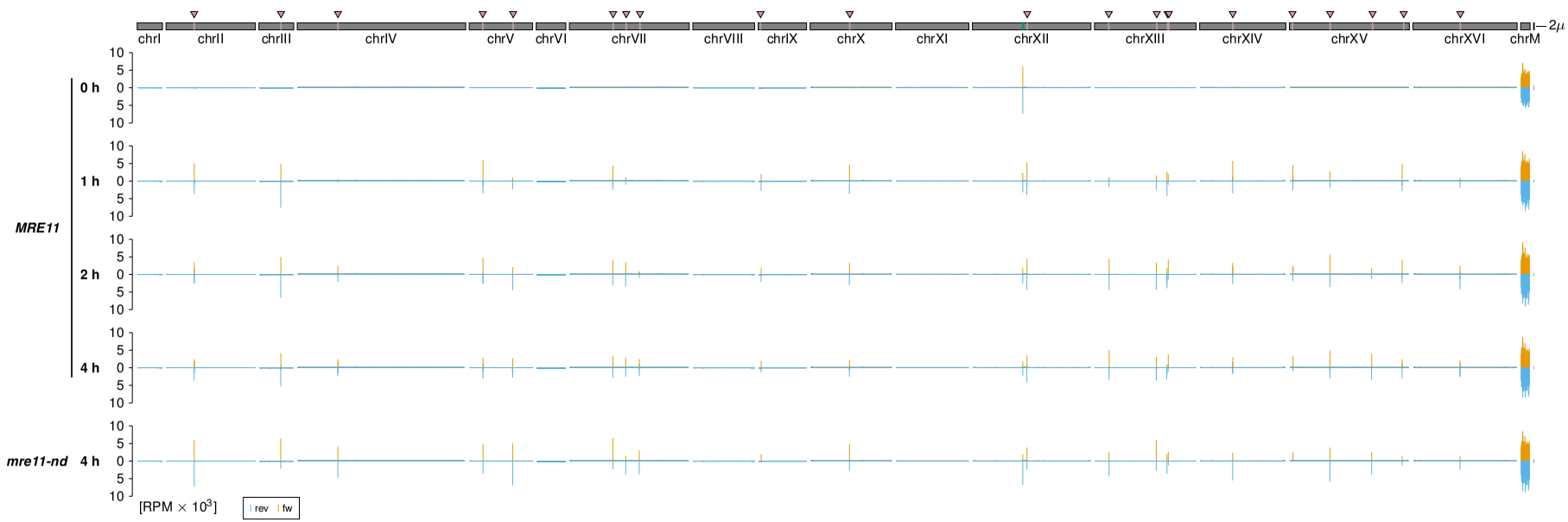
chrI
chrII
chrIII
chrIV
chrV
chrVI
chrVII
chrVIII
chrIX
chrX
chrXI
chrXII
chrXIII
chrXIV
chrXV
chrXVI
chrM
2μ
MRE11
0 h
1 h
2 h
4 h
mre11-nd
4 h
10
5
0
5
10
[RPM × 10^3]
rev
fw

Figure S2: Genome-wide S1-seq coverage, related to Figure 1

S1-seq coverage in 1-kb bins is plotted along *S. cerevisiae* chromosomes, mitochondrial DNA (chrM), and the 2-micron plasmid (2μ). On top, chromosomes (gray bars) and SrfI cut site locations (pink lines and triangles) are plotted to scale. Note the DSB-independent S1-seq signal (0 h) at the ribosomal DNA locus (green line on chrXII) and chrM. Also note that S1-seq coverage is absent at telomere ends because we filtered out reads with non-unique mapping (equal alignment score for best and second-best mapping). RPM: reads per million reads.

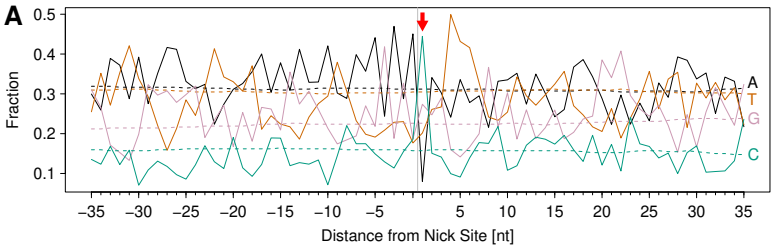
A
Fraction
Distance from Nick Site [nt]

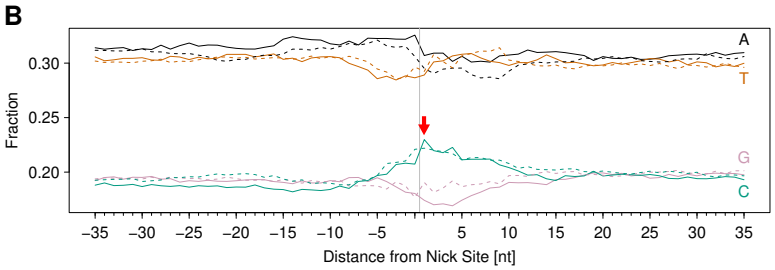
B
Fraction
Distance from Nick Site [nt]

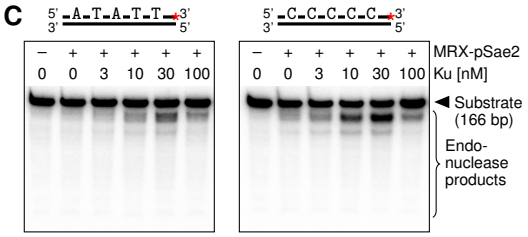
C
MRX-pSae2
Ku [nM]
Substrate (166 bp)
Endo-nuclease products

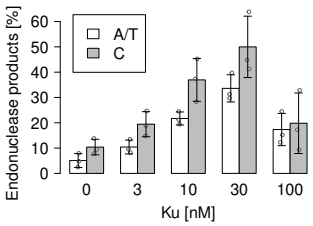
D
Endonuclease products [%]
A/T
C
Ku [nM]

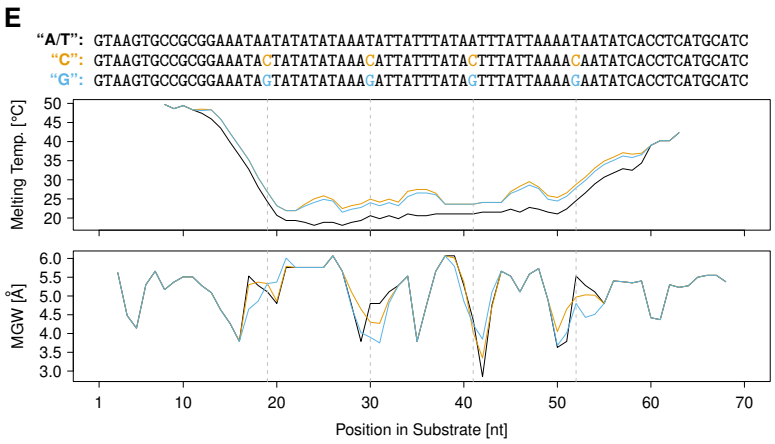
E
"A/T": GTAAGTGCCGCGGAAATAATATATATAAATATTATTTATAATTTATTAAAATAATATCACCTCATGCATC
"C": GTAAGTGCCGCGGAAATACTATATATAAACATTATTTATACTTTATTAAAACAATATCACCTCATGCATC
"G": GTAAGTGCCGCGGAAATAGTATATATAAAGATTATTTATAGTTTATTAAAAGAATATCACCTCATGCATC
Melting Temp. [°C]
MGW [Å]
Position in Substrate [nt]

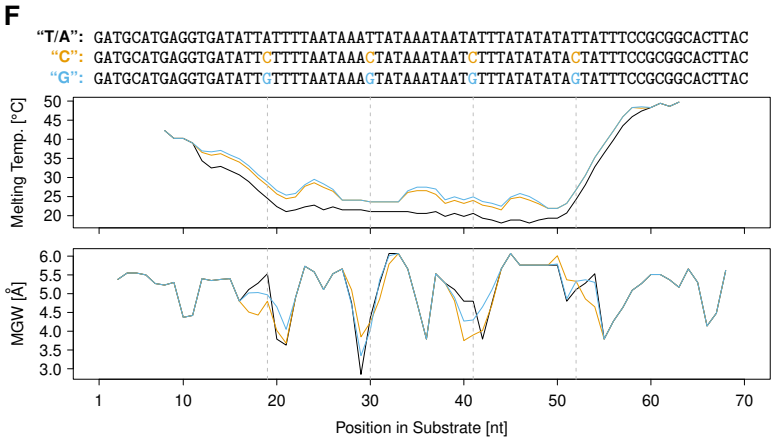
F
"T/A": GATGCATGAGGTGATATTATTTTTAATAAATTATAAATAATATTTATATATATTATTTCCGCGGCACTTAC
"C": GATGCATGAGGTGATATTCTTTTAATAAACTATAAATAATCTTTATATATACTATTTCCGCGGCACTTAC
"G": GATGCATGAGGTGATATTGTTTTAATAAAGTATAAATAATGTTTATATATAGTATTTCCGCGGCACTTAC
Melting Temp. [°C]
MGW [Å]
Position in Substrate [nt]

Figure S3: MRX preferentially nicks at a specific sequence motif, related to Figure 3

(A) *exo1*Δ *sgs1*Δ data from (Bazzano et al., 2021), containing MRX nicking information in a 300-bp region upstream of a single DSB, were analyzed as shown in Figure 3A. Color-coded solid and dashed lines show nicking preference (average weighted with coverage scores) and background (unweighted average), respectively. The vertical gray line indicates the nick site and the red arrow highlights the increased C fraction.

(B) Wild-type (WT) and *exo1* nuclease-dead (*exo1-nd*) data from (Mimitou et al., 2017), containing resection tract end points next to meiotic DSBs, were analyzed. Only loner Spo11 hotspots (neighboring hotspots at least 3 kb away) were considered. Color-coded solid and dashed lines indicate data from *exo1-nd* (where resection is solely due to MRX nicking) and WT strains (where resection end points derive from a combination of MRX nicking and Exo1-mediated resection), respectively. The vertical gray line indicates the nick site or resection end point for *exo1-nd* and WT, respectively, and the red arrow highlights the increased C fraction. Note that S1-seq also detected unprocessed Spo11-bound DSBs and recombination intermediates in this dataset, which might impact on the observed nucleotide fractions (Mimitou et al., 2017).

(C) *In vitro* MRX nicking in the presence of various concentrations of the yeast Ku complex with substrates containing (right panel) or lacking positioned Cs (left panel). The substrate structures are shown on top, and the red asterisks indicate the position of the radioactive label. Note that longer DNA substrates were used as compared to Fig. 3 to avoid that Ku bound at the opposite end might influence the nick positions. The first 53 bp are identical to the substrates used in Fig. 3.

(D) Quantification of nicking assays such as shown in (C). Individual values (circles) and means (bar heights) ± SD (error bars) of three independent replicates are shown.

(E) Melting temperature and minor groove width (MGW) along the DNA substrates used in Fig. 3C-G (top strand).

(F) Melting temperature and minor groove width (MGW) along the DNA substrates used in Fig. 3C-D (bottom strand).

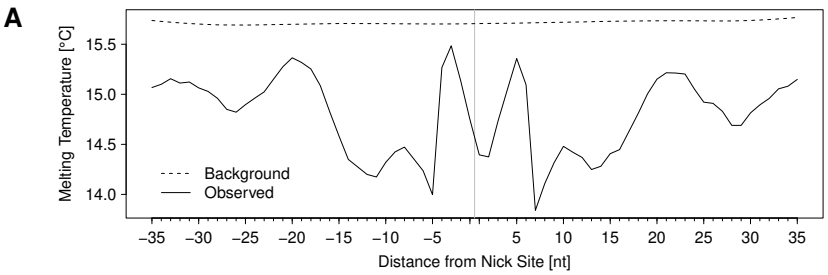
A
Melting Temperature [°C]
15.5
15.0
14.5
14.0
Background
Observed
−35 −30 −25 −20 −15 −10 −5 5 10 15 20 25 30 35
Distance from Nick Site [nt]

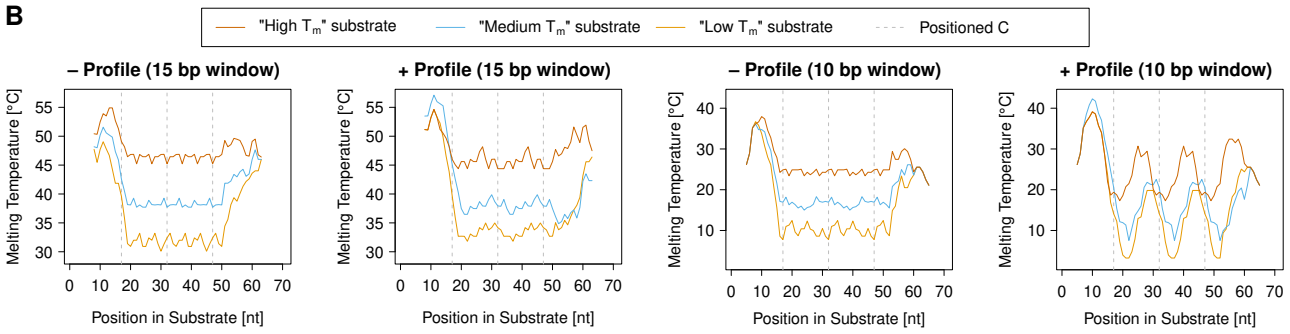
B
"High Tm" substrate
"Medium Tm" substrate
"Low Tm" substrate
Positioned C
– Profile (15 bp window)
+ Profile (15 bp window)
– Profile (10 bp window)
+ Profile (10 bp window)
Melting Temperature [°C]
Position in Substrate [nt]

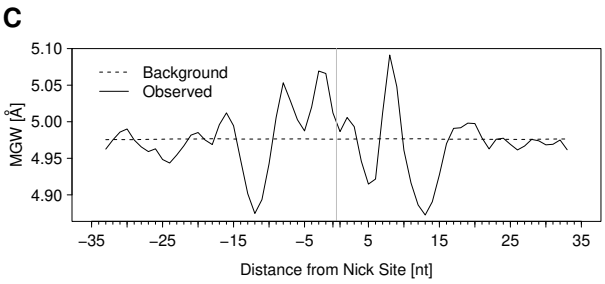
C
MGW [Å]
5.10
5.05
5.00
4.95
4.90
Background
Observed
−35 −25 −15 −5 5 15 25 35
Distance from Nick Site [nt]

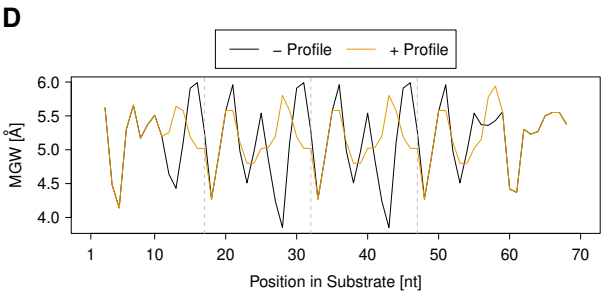
D
– Profile
+ Profile
MGW [Å]
6.0
5.5
5.0
4.5
4.0
1 10 20 30 40 50 60 70
Position in Substrate [nt]

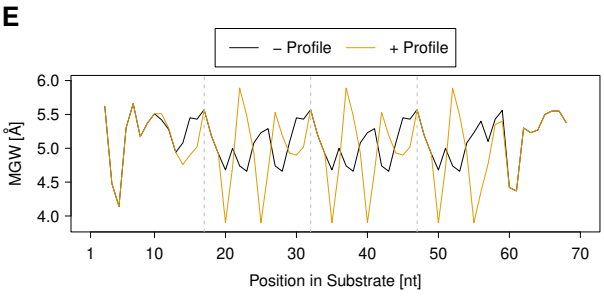
E
– Profile
+ Profile
MGW [Å]
6.0
5.5
5.0
4.5
4.0
1 10 20 30 40 50 60 70
Position in Substrate [nt]

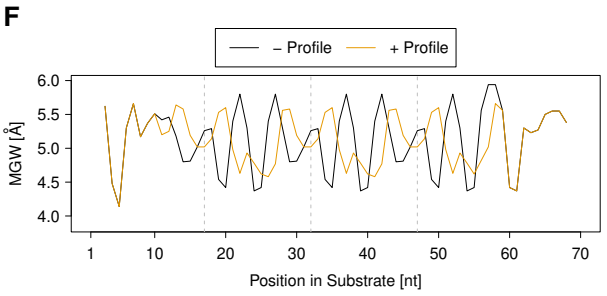
F
– Profile
+ Profile
MGW [Å]
6.0
5.5
5.0
4.5
4.0
1 10 20 30 40 50 60 70
Position in Substrate [nt]

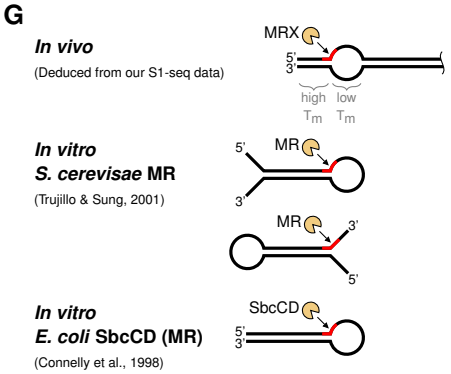
G
In vivo
(Deduced from our S1-seq data)
MRX
5'
3'
high Tm
low Tm
In vitro
S. cerevisae MR
(Trujillo & Sung, 2001)
5'
MR
3'
MR
3'
5'
In vitro
E. coli SbcCD (MR)
(Connelly et al., 1998)
SbcCD
5'
3'

Figure S4: MRX preferentially nicks DNA with a specific melting temperature profile, related to Figure 4
(A) Melting temperature at indicated distance from the MRX nick site (vertical gray line). Solid and dashed black lines show nicking preference (average weighted with S1-seq score) and background (unweighted average), respectively. Melting temperatures were calculated for 10-bp windows centered at the indicated distance.
(B) Melting temperature profiles of the *in vitro* substrates used in Fig. 4C-D. Window sizes for melting temperature calculations are indicated.
(C) Minor groove width (MGW) at indicated distance from the MRX nick site (vertical gray line) for MRX *in vivo* nicking. The solid and dashed black lines show the nicking preference (average weighted with S1-seq score) and background (unweighted average), respectively.
(D-F) Minor groove width (MGW) calculated along the DNA substrates used in Fig. 4C-D with low (D), medium (E), and high (F) overall melting temperature.
(G) The proposed melted DNA structure *in vivo* (top) is aligned with the substrates used in *in vitro* assays as reported in (Trujillo and Sung, 2001) and (Connelly et al., 1998). Corresponding ss/dsDNA junctions are highlighted in red and the dominant nicking sites are indicated. For the *in vivo* structure, regions of high and low melting temperature (T_m) are indicated.

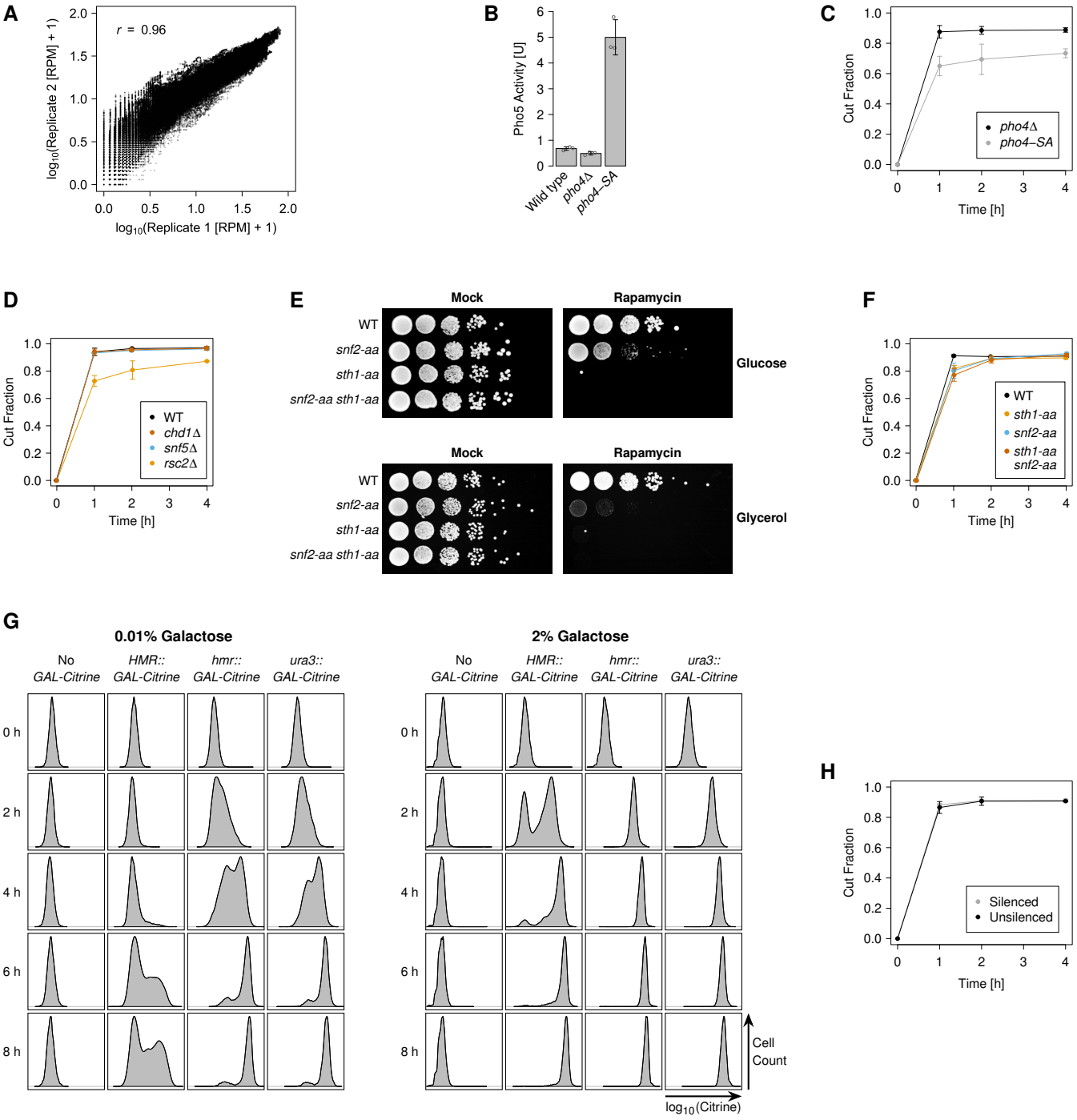
A
r = 0.96
log10(Replicate 2 [RPM] + 1)
log10(Replicate 1 [RPM] + 1)
B
Pho5 Activity [U]
Wild type
pho4Δ
pho4–SA
C
Cut Fraction
pho4Δ
pho4–SA
Time [h]
D
Cut Fraction
WT
chd1Δ
snf5Δ
rsc2Δ
Time [h]
E
Mock
Rapamycin
WT
snf2-aa
sth1-aa
snf2-aa sth1-aa
Glucose
Glycerol
F
Cut Fraction
WT
sth1-aa
snf2-aa
sth1-aa snf2-aa
Time [h]
G
0.01% Galactose
2% Galactose
No GAL-Citrine
HMR:: GAL-Citrine
hmr:: GAL-Citrine
ura3:: GAL-Citrine
0 h
2 h
4 h
6 h
8 h
Cell Count
log10(Citrine)
H
Cut Fraction
Silenced
Unsilenced
Time [h]

Figure S5: Impact of nucleosomes and heterochromatin on MRX nicking, related to Figure 5

(A) Reproducibility of MNase-seq assays. MNase-seq scores at each nucleotide position in ± 2 kbp regions around all DSBs are plotted for two biological replicates (0, 1, 2, and 4 h after SrfI induction). The Pearson's correlation coefficient r is specified.

(B) Pho5 activity associated with cells of the indicated genotypes. See methods section for assay description and unit definition. Individual values (circles) and means (bar heights) ± SD (error bars) of three biological replicates are shown.

(C) DSB formation kinetics related to Figure 5D. DSB formation at the SrfI cut site engineered into the *PHO5* promoter was monitored in the indicated strains. Data are represented as mean ± SD of three biological replicates.

(D) DSB formation kinetics related to Figure 5E. DSB formation at the *MAT*a HO cut site was monitored in the indicated strains. Data are represented as mean ± SD of three biological replicates.

(E) Viability of the indicated strains in the presence of 1 μg/ml Rapamycin or mock control (1‰ DMSO). Exponentially growing cells were spotted in a 1:10 dilution series on solid YP media containing the indicated carbon source. As expected, anchoring away Sth1 leads to inviability (Laurent et al., 1992), while anchoring away Snf2 leads to reduced growth, especially when glycerol is the sole carbon source (Neigeborn & Carlson, 1984). Note that the used strains lack *dna2-aa* to prevent Rapamycin-induced inviability due to anchoring away Dna2. A representative example of three biological replicates is shown.

(F) DSB formation kinetics related to Figure 5F. DSB formation at *MAT*a *hocs::SrfIcs* was monitored in the indicated strains. Data are represented as mean ± SD of three biological replicates.

(G) Galactose induction of a P_{GAL1}-*Citrine* reporter gene inserted into the *HMR* locus is delayed and suppressed if *HMR* silencing seed sequences are present (*HMR::GAL-Citrine*), but not if they are absent (*hmr::GAL-Citrine*). A background strain (No *GAL-Citrine*) and a strain with the reporter inserted at the unrelated (unsilenced) *URA3* locus (*ura3::GAL-Citrine*) were used as controls. Upon addition of the indicated galactose concentrations, samples were analyzed by flow cytometry at the indicated time points. Citrine fluorescence distributions in the cell populations are plotted. A representative example of three biological replicates is shown. Note the bimodal distributions for low galactose concentrations and/or early time points, which has been observed before and ascribed to the feedback loops in the *GAL* network, resulting in all-or-nothing gene induction (Acar et al., 2005).

(H) DSB formation kinetics related to Figure 5H. DSB formation at the HO cut site engineered downstream of *HMR* was monitored in the indicated strains. Data are represented as mean ± SD of three biological replicates.

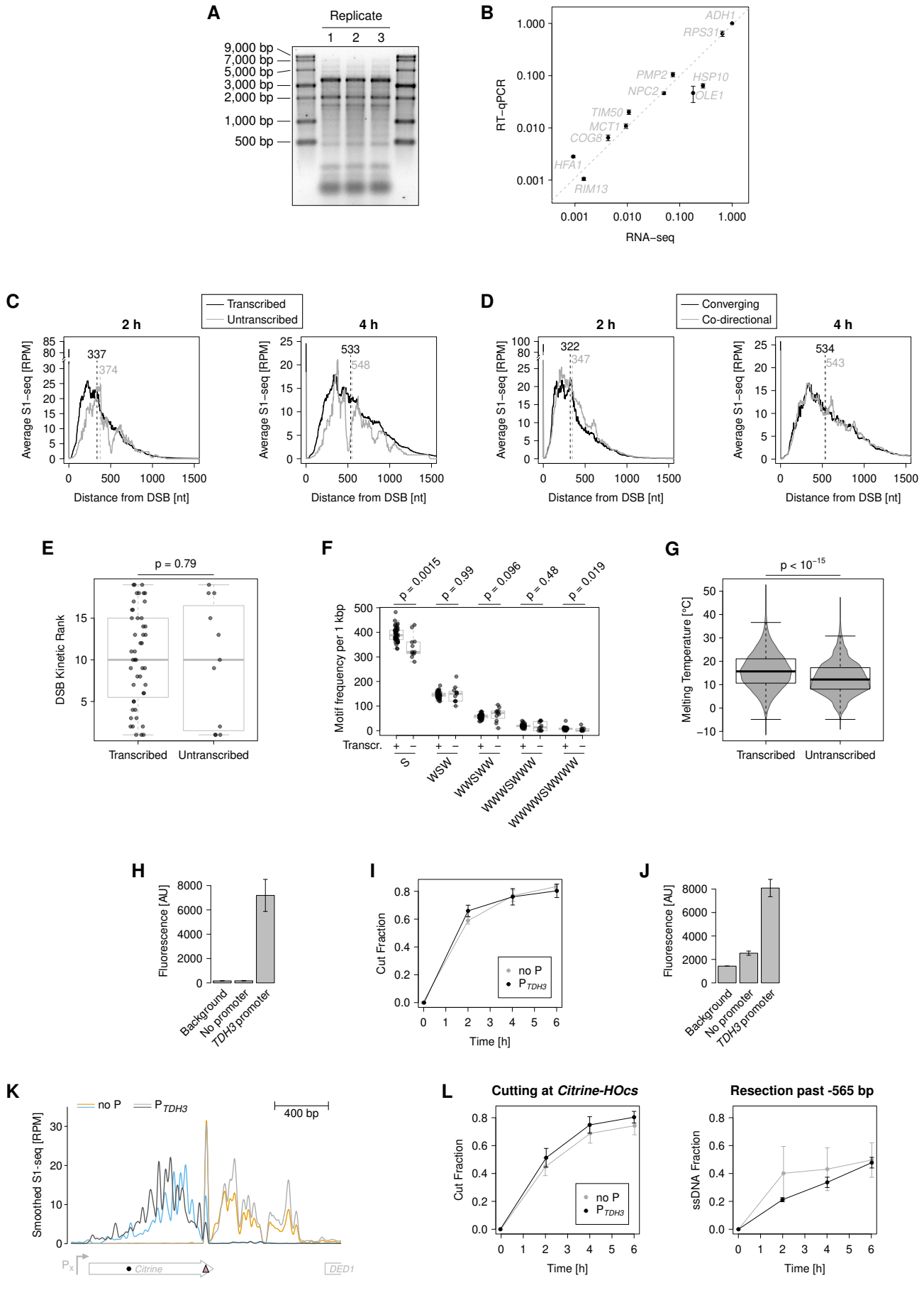
A
Replicate
1 2 3
9,000 bp
7,000 bp
5,000 bp
3,000 bp
2,000 bp
1,000 bp
500 bp
B
RT−qPCR
RNA−seq
ADH1
RPS31
PMP2
HSP10
NPC2
OLE1
TIM50
MCT1
COG8
HFA1
RIM13
C
Transcribed
Untranscribed
2 h
4 h
Average S1−seq [RPM]
Distance from DSB [nt]
337
374
533
548
D
Converging
Co-directional
322
347
534
543
E
p = 0.79
DSB Kinetic Rank
Transcribed
Untranscribed
F
p = 0.0015
p = 0.99
p = 0.096
p = 0.48
p = 0.019
Motif frequency per 1 kbp
Transcr.
S
WSW
WWSWW
WWWSWWW
WWWWSWWWW
G
p < 10−15
Melting Temperature [°C]
H
Fluorescence [AU]
Background
No promoter
TDH3 promoter
I
Cut Fraction
Time [h]
no P
P TDH3
J
K
Smoothed S1-seq [RPM]
400 bp
Citrine
DED1
L
Cutting at Citrine-HOcs
Resection past -565 bp
ssDNA Fraction

Figure S6: Transcription impedes MRX nicking, related to Figure 6

(A) Total RNA samples (500 ng) were denatured, subjected to electrophoresis on a 1×TBE 1.5% agarose gel, and stained with 1×SYBR Gold. The sharpness of the 25S and 18S ribosomal RNA bands (ca. 3.5 and 2 kbp, respectively) indicate good RNA integrity.

(B) Confirmation of transcription levels next to DSB formation sites. Reverse Transcription (RT)-qPCR-derived transcript levels (normalized to the *ADH1* transcript level) are plotted verses RNA-seq-derived transcript levels (averaged over the CDS and normalized to the *ADH1* transcript level) from the (Maya-Miles et al., 2019) dataset. Data are represented as mean ± SD of three biological replicates. Gene names are indicated. The gray dashed line shows a linear regression. The equation of the regression line is RT-qPCR $= 0.00006 + 1.001 \cdot$ RNA-seq and the regression coefficient is $R^2 = 0.9993$, confirming an excellent linear correlation and the applicability of the RNA-seq data set to our strains and culture conditions.

(C) Average 51-nt smoothed S1-seq coverage spreading from all DSBs 2 h and 4 h post SrfI induction grouped by transcriptional activity. Numbers above vertical dashed lines indicate average spreading distance from DSBs.

(D) Average 51-nt smoothed S1-seq coverage spreading from all DSBs 2 h and 4 h post SrfI induction in transcribed regions grouped by converging or co-directional orientation of transcription and resection. Numbers above vertical dashed lines indicate average spreading distance from DSBs.

(E) DSB formation kinetics of transcribed and untranscribed regions. Data are represented as individual values (derived from Figure S1B) for all DSB-proximal transcribed and untranscribed regions and summarized as box plots. A Mann-Whitney-Wilcoxon test was used to test for a statistically significant difference and the p-value is indicated.

(F) Motif frequencies in transcribed and untranscribed regions. Data are represented as individual values for all DSB-proximal transcribed and untranscribed regions and summarized as box plots. Motif sequences are represented as IPUAC codes (W: A or T; S: G or C). Mann-Whitney-Wilcoxon tests were used to test for statistically significant differences and the p-values are indicated.

(G) Local melting temperatures (10-bp windows) of transcribed and untranscribed regions. Data were calculated for each nucleotide along all DSB-proximal transcribed and untranscribed regions and represented as bean plots and summarized as box plots. A Mann-Whitney-Wilcoxon test was used to test for a statistically significant difference and the p-value is indicated.

(H) mKate2 fluorescence as measured by flow cytometry in strains containing the P_x-*mKate2-HOcs* reporter construct. Data are represented as mean ± SD of three biological replicates.

(I) DSB formation kinetics related to Figure 6E. DSB formation at the P_x-*mKate2-HOcs* reporter construct was monitored in the indicated strains. Data are represented as mean ± SD of three biological replicates.

(J) Citrine fluorescence as measured by flow cytometry in strains containing the P_x-*Citrine-HOcs* reporter construct. Data are represented as mean ± SD of three biological replicates.

(K) 51-nt smoothed S1-seq coverage 2 h post DSB induction around the HO cut site (pink filled triangle) located near the 3' end of the Citrine reporter gene. The filled circle indicates the site where resection was evaluated using a qPCR-based assay, as shown in (L).

(L) (Left panel) DSB formation at the P_x-*Citrine-HOcs* reporter construct. (Right panel) Resection was evaluated at -565 bp from the DSB, as also indicated in (K). Data are represented as mean ± SD of three biological replicates.

Table S1: DNA oligos for the *in vitro* nicking assay substrates, related to Key Resources Table of STAR methods section

The forward strand was radioactively labeled, unless stated otherwise.
[a]Dir.: Direction (fw: forward, rev: reverse). [b]`[BioT]`: biotin-dT.

Substrate/ Name	Dir.[a]	Sequence[b]
A/T	fw	GTAAGTGCCGCGGAAATAATATATATAAATATTATTTATAATTTATTAAAATAATATCACCTCATGCATC
	rev	GATGCATGAGGTGATATTATTTTAATAAATTATAAATAATATTTATATATATTATTTCCGCGGCACTTAC
C	fw	GTAAGTGCCGCGGAAATACTATATATAAACATTATTTATACTTTATTAAAACAATATCACCTCATGCATC
	rev	GATGCATGAGGTGATATTGTTTTAATAAAGTATAAATAATGTTTATATATAGTATTTCCGCGGCACTTAC
G	fw	GTAAGTGCCGCGGAAATAGTATATATAAAGATTATTTATAGTTTATTAAAAGAATATCACCTCATGCATC
	rev	GATGCATGAGGTGATATTCTTTTAATAAACTATAAATAATCTTTATATATACTATTTCCGCGGCACTTAC
Low T_m + Profile	fw	GTAAGTGCCGCGTGGACATTAATATTGTGGACATTAATATTGTGGACATTAATATTGCACCTCATGCATC
	rev	GATGCATGAGGTGCAATATTAATGTCCACAATATTAATGTCCACAATATTAATGTCCACGCGGCACTTAC
Low T_m – Profile	fw	GTAAGTGCCGCGTTTACATTAGGATAGTTTACATTAGGATAGTTTACATTAGGATAGCACCTCATGCATC
	rev	GATGCATGAGGTGCTATCCTAATGTAAACTATCCTAATGTAAACTATCCTAATGTAAACGCGGCACTTAC
Medium T_m + Profile	fw	GTAAGTGCCGCGGGGACAAGATAAGATGGGACAAGATAAGATGGGACAAGATAAGATCACCTCATGCATC
	rev	GATGCATGAGGTGATCTTATCTTGTCCCATCTTATCTTGTCCCATCTTATCTTGTCCCCGCGGCACTTAC
Medium T_m – Profile	fw	GTAAGTGCCGCGATGACAAGAGATGAGATGACAAGAGATGAGATGACAAGAGATGAGCACCTCATGCATC
	rev	GATGCATGAGGTGCTCATCTCTTGTCATCTCATCTCTTGTCATCTCATCTCTTGTCATCGCGGCACTTAC
High T_m + Profile	fw	GTAAGTGCCGCGTGGACATAGGAGGGGTGGACATAGGAGGGGTGGACATAGGAGGGGCACCTCATGCATC
	rev	GATGCATGAGGTGCCCCTCCTATGTCCACCCCTCCTATGTCCACCCCTCCTATGTCCACGCGGCACTTAC
High T_m – Profile	fw	GTAAGTGCCGCGAGGACAGGTGAGGTGAGGACAGGTGAGGTGAGGACAGGTGAGGTGCACCTCATGCATC
	rev	GATGCATGAGGTGCACCTCACCTGTCCTCACCTCACCTGTCCTCACCTCACCTGTCCTCGCGGCACTTAC
A/T long	fw	GTAAGTGCCGCGGAAATAATATATATAAATATTATTTATAATTTATTAAAATATTATATTATTTATTATA TATTAATATATATTTAAAATTTAAATTTATATTTAATATAATGGGTGCCAGGGCGTGCCCTTGGGCTCCC CGGGCGCGTACTCCACCTCATGCATC
	rev	GATGCATGAGGTGGAGTACGCGCCCGGGGAGCCCAAGGGCACGCCCTGGCACCCATTATATTAAATATAA ATTTAAATTTTAAATATATATTAATATATAATAAATAATATAATATTTTAATAAATTATAAATAATATTT ATATATATTATTTCCGCGGCACTTAC
C long	fw	GTAAGTGCCGCGGAAATACTATATATAAACATTATTTATACTTTATTAAAACATTATATTATCTATTATA TATCAATATATATTCAAAATTTAAACTTATATTTAACATAATGGGTGCCAGGGCGTGCCCTTGGGCTCCC CGGGCGCGTACTCCACCTCATGCATC
	rev	GATGCATGAGGTGGAGTACGCGCCCGGGGAGCCCAAGGGCACGCCCTGGCACCCATTATGTTAAATATAA GTTTAAATTTTGAATATATATTGATATATAATAGATAATATAATGTTTTAATAAAGTATAAATAATGTTT ATATATAGTATTTCCGCGGCACTTAC
PC210	fw	G`[BioT]`AAGTGCCGCGGTGCGGGTGCCAGGGCGTGCCCTTGGGCTCCCCGGGCGCGTACTCCACCTCAT GCA`[BioT]`C
PC211	rev	GA`[BioT]`GCATGAGGTGGAGTACGCGCCCGGGGAGCCCAAGGGCACGCCCTGGCACCCGCACCGCGGCA CT`[BioT]`AC

Table S2: Quantitative PCR primers used in this study, related to Key Resources Table of STAR methods section

[a]Dir.: Direction (fw: forward, rev: reverse).

Name	Amplicon	Dir.[a]	Sequence
oRG46	*MAT*a HO cut site (*HOcs*)	fw	TCAATGATTAAAATAGCATAGTCGGGT
oRG47	*MAT*a *HOcs*	rev	CGTCAACCACTCTACAAAACCA
oRG50	RsaI cut site (*RsaIcs*) @ *HOcs* +98 bp	fw	TGGTGACGGATATTGGGAAGA
oRG51	*RsaIcs* @ HOcs +98 bp	rev	CGCCACGACCACACTCTATA
oRG52	*RsaIcs* @ HOcs +640 bp	fw	ACTTATCTTTATCTTATTCGCCTTCTTG
oRG53	*RsaIcs* @ HOcs +640 bp	rev	GAGAAGACTTGTGGCGAAGA
oRG54	*ADH1*	fw	GTTAAGGGCTGGAAGATCGG
oRG55	*ADH1*	rev	TTGTTGGAAAGAACCGTCGT
oRG341	*SrfIcs* @ chrII:256173	fw	CCTTGACTTTTAGCGTGGAAGA
oRG342	*SrfIcs* @ chrII:256173	rev	TGGCCATTGTTTGCGTTTATAT
oRG496	*HMR-HOcs* (@ chrIII:295659)	fw	GTGACACCCAGGTTGCCG
oRG497	*HMR-HOcs* (@ chrIII:295659)	rev	AATGTCATCAAAAGGCGGCC
oRG641	*mKate2-T_{CYC2}-HOcs*	fw	ACGTGTAGTAACTCTTTGAAGCT
oRG642	*mKate2-T_{CYC2}-HOcs*	rev	TGATTACGCCAAGCTCGAAA
oRG645	*Citrine-HOcs-HA*	fw	CCAAAGATCCAAACGAAAAGAGA
oRG646	*Citrine-HOcs-HA*	rev	GCCTGTCTCGAGTTAAGCGT
oRG709	AluI cut site (*AluIcs*) @ *mKate2-T_{CYC2}(242 bp)-HOcs* -431 bp	fw	ATTGGTTGGTGGTGGTCATT
oRG710	*AluIcs* @ *mKate2-T_{CYC2}(242 bp)-HOcs* -431 bp	rev	CAACGTAATAAACACCTGGCATT
oRG711	*AluIcs* @ *mKate2-T_{CYC2}(153 bp)-HOcs* -435 bp	fw	CTGATGGTGGTTTGGAAGGT
oRG712	*AluIcs* @ *mKate2-T_{CYC2}(153 bp)-HOcs* -435 bp	rev	CCACCAACCAATTTCAAAGC
oRG721	StyI cut site (*StyIcs*) @ *Citrine-HOcs* -591 bp	fw	TTTCTGTCTCCGGTGAAGGT
oRG722	*StyIcs* @ *Citrine-HOcs* -591 bp	rev	GGCATGGCAGACTTGAAAAA
oRG723	*AluIcs* @ *Citrine-hisG-HOcs* -542 bp	fw	GCCATGCCAGAAGGTTATGT
oRG724	*AluIcs* @ *Citrine-hisG-HOcs* -542 bp	rev	ATTCCAATTTGTGACCTAAAATGT
oRG790	*P_{PHO5}*-SrfI cut site (*SrfIcs*)	fw	GCAGCGCACATAAGATGACT
oRG791	*P_{PHO5}-SrfIcs*	rev	GTCGCACGCTCTCTTTACAG
oRG802	MseI cut site (*MseIcs*) @ *P_{PHO5}-SrfIcs* -223 bp	fw	GTGTGAGTGCCAAGGTTGTA
oRG803	*MseIcs* @ *P_{PHO5}-SrfIcs* -223 bp	rev	TTTTCGCATAGAACGCAACTG
oRG806	*MseIcs* @ *P_{PHO5}-SrfIcs* -538 bp	fw	AGAGTAGTATGGTCCGGCAC
oRG807	*MseIcs* @ *P_{PHO5}-SrfIcs* -538 bp	rev	GCGCTGATGTTTTGCTAAGTC
oRG808	*MseIcs* @ *HMR-HOcs* -607 bp	fw	TTCCTAAAGTGTTGCCAGCG
oRG809	*MseIcs* @ *HMR-HOcs* -607 bp	rev	TCCGGGTCTGGTAATGGATG
oRG876	*COG8*	fw	GCAAAGTGGAAGGCGAAGAT
oRG877	*COG8*	rev	TCAGCCTTGTCTTCTGTTTTGT
oRG878	*HFA1*	fw	ACAGAGCAGTAGTGGAGTTCA
oRG879	*HFA1*	rev	TGTCCACCAACCTAGTTAGCT
oRG882	*HSP10*	fw	ACCGTGTCCTTGTCCAAAGA
oRG883	*HSP10*	rev	CCTACGGCAACAACTTCAGC
oRG888	*MCT1*	fw	CCGGTCTGGTTGATGATTTAGAG
oRG889	*MCT1*	rev	GGAAGGGGATGTTGTATGGG
oRG892	*NPC2*	fw	CCCACCAAACACCAAACCAA
oRG893	*NPC2*	rev	AGACCTCACCGTTAGCAGAA
oRG896	*OLE1*	fw	GACAGAAGAACCCCTCGTGA
oRG897	*OLE1*	rev	CAGTTGGGAATTCGTGGTGG
oRG898	*PMP2*	fw	TGATGAGCACGTTACCAGGT
oRG899	*PMP2*	rev	TGGTAGAAATGATGGCGATACA
oRG903	*RIM13*	fw	CCTTAAACAAGACGTGCCCA
oRG904	*RIM13*	rev	CCGTATCGAGGCAAGCAATT
oRG907	*RPS31*	fw	TGAGATTGAGAGGTGGTGGT
oRG908	*RPS31*	rev	ACCTTCAGCATCGACCTTGT
oRG909	*TIM50*	fw	CAAGTTCCCGCTCGATTTGA
oRG910	*TIM50*	rev	TAAATGTTTGCCCGCCCATT

Table S3: Adapter and primer oligonucleotides used for deep-sequencing library preparation, related to Key Resources Table of STAR methods section

[a]Dir.: Direction (fw: forward, rev: reverse). [b]Modified bases are denoted as follows: /5Phos/: 5'-phosphate, N: random nucleotide, /3InvdT/: 3' inverted Thymidine, *: phosphorothioate bond, and /5BiosG/: 5' Biotin. Lowercase letters indicate barcode indices.

Name	Target/Usage	Dir.[a]	Sequence[b]
oRG462	1st adapter (P5) – version 1	rev	/5Phos/CGTCTGCAGNNNNNNNNNNNNAGATCGGAAGAGCGTCGTG/3InvdT/
oRG463	1st adapter (P5) – version 1	fw	/5BiosG/CACGACGCTCTTCCGATCTNNNNNNNNNNNNCTGCAGACG*T
oRG316	2nd adapter (P7) – version 1	fw	/5Phos/GATCGGAAGAGCACACGTCTGAACTCCAGTCAC/3InvdT/
oRG464	2nd adapter (P7) – version 1	rev	GTGACTGGAGTTCAGACGTGTGCTCTTCCGATC*T
oRG729	1st adapter (P5) – version 2 & 3	fw	/5BiosG/ACACTCTTTCCCTACACGACGCTCTTCCGATC*T
oRG730	1st adapter (P5) – version 2 & 3	rev	/5Phos/GATCGGAAGAGCGTCGTGTAGGGAAAGAGTGT/3InvdT/
oRG731	2nd adapter (P7) – version 2	fw	/5Phos/GTAGCGTAGAGCNNNNNNNNNNNNAGATCGGAAGAGCACACGTCTGAACTCCAGTCAC/3InvdT/
oRG732	2nd adapter (P7) – version 2	rev	GTGACTGGAGTTCAGACGTGTGCTCTTCCGATCTNNNNNNNNNNNNGCTCTACGCTAC*T
oRG816	2nd adapter (P7) #1 – version 3	fw	/5Phos/GTCACTGAGCATNNNNNNNNNNNNAGATCGGAAGAGCACACGTCTGAACTCCAGTCAC/3InvdT/
oRG817	2nd adapter (P7) #1 – version 3	rev	GTGACTGGAGTTCAGACGTGTGCTCTTCCGATCTNNNNNNNNNNNNATGCTCAGTGAC*T
oRG818	2nd adapter (P7) #2 – version 3	fw	/5Phos/TCAGTACGAGTCNNNNNNNNNNNNAGATCGGAAGAGCACACGTCTGAACTCCAGTCAC/3InvdT/
oRG819	2nd adapter (P7) #2 – version 3	rev	GTGACTGGAGTTCAGACGTGTGCTCTTCCGATCTNNNNNNNNNNNNGACTCGTACTGA*T
oRG820	2nd adapter (P7) #3 – version 3	fw	/5Phos/CAGCAGTCTTGANNNNNNNNNNNNAGATCGGAAGAGCACACGTCTGAACTCCAGTCAC/3InvdT/
oRG821	2nd adapter (P7) #3 – version 3	rev	GTGACTGGAGTTCAGACGTGTGCTCTTCCGATCTNNNNNNNNNNNNTCAAGACTGCTG*T
oRG822	2nd adapter (P7) #4 – version 3	fw	/5Phos/AGTTGCATCACGNNNNNNNNNNNNAGATCGGAAGAGCACACGTCTGAACTCCAGTCAC/3InvdT/
oRG823	2nd adapter (P7) #4 – version 3	rev	GTGACTGGAGTTCAGACGTGTGCTCTTCCGATCTNNNNNNNNNNNNCGTGATGCAACT*T
oRG827	TrueSeq Universal adapter 3' part	fw	ACACTCTTTCCCTACACGACGCTCTTCCGATC*T
oRG828	TrueSeq Universal adapter 3' part	rev	/5Phos/GATCGGAAGAGCACACGTCTGAACTCCAGTCAC
oRG318	TrueSeq Adapter (P5)	fw	AATGATACGGCGACCACCGAGATCTACACTCTTTCCCTACACGACGCTCTTCCGATCT
oRG757	TrueSeq Adapter (P7), Index 1	rev	CAAGCAGAAGACGGCATACGAGATcgtgatGTGACTGGAGTTCAGACGTGTG
oRG758	TrueSeq Adapter (P7), Index 2	rev	CAAGCAGAAGACGGCATACGAGATacatcgGTGACTGGAGTTCAGACGTGTG
oRG498	TrueSeq Adapter (P7), Index 3	rev	CAAGCAGAAGACGGCATACGAGATgcctaaGTGACTGGAGTTCAGACGTGTG
oRG319	TrueSeq Adapter (P7), Index 4	rev	CAAGCAGAAGACGGCATACGAGATtggtcaGTGACTGGAGTTCAGACGTGTG
oRG320	TrueSeq Adapter (P7), Index 5	rev	CAAGCAGAAGACGGCATACGAGATcactgtGTGACTGGAGTTCAGACGTGTG
oRG321	TrueSeq Adapter (P7), Index 6	rev	CAAGCAGAAGACGGCATACGAGATattggcGTGACTGGAGTTCAGACGTGTG
oRG322	TrueSeq Adapter (P7), Index 7	rev	CAAGCAGAAGACGGCATACGAGATgatctgGTGACTGGAGTTCAGACGTGTG
oRG759	TrueSeq Adapter (P7), Index 8	rev	CAAGCAGAAGACGGCATACGAGATtcaagtGTGACTGGAGTTCAGACGTGTG
oRG760	TrueSeq Adapter (P7), Index 9	rev	CAAGCAGAAGACGGCATACGAGATctgatcGTGACTGGAGTTCAGACGTGTG
oRG761	TrueSeq Adapter (P7), Index 10	rev	CAAGCAGAAGACGGCATACGAGATaagctaGTGACTGGAGTTCAGACGTGTG
oRG762	TrueSeq Adapter (P7), Index 11	rev	CAAGCAGAAGACGGCATACGAGATgtagccGTGACTGGAGTTCAGACGTGTG
oRG763	TrueSeq Adapter (P7), Index 12	rev	CAAGCAGAAGACGGCATACGAGATtacaagGTGACTGGAGTTCAGACGTGTG
oRG764	TrueSeq Adapter (P7), Index 13	rev	CAAGCAGAAGACGGCATACGAGATttgactGTGACTGGAGTTCAGACGTGTG
oRG765	TrueSeq Adapter (P7), Index 14	rev	CAAGCAGAAGACGGCATACGAGATggaactGTGACTGGAGTTCAGACGTGTG
oRG766	TrueSeq Adapter (P7), Index 15	rev	CAAGCAGAAGACGGCATACGAGATtgacatGTGACTGGAGTTCAGACGTGTG
oRG767	TrueSeq Adapter (P7), Index 16	rev	CAAGCAGAAGACGGCATACGAGATggacggGTGACTGGAGTTCAGACGTGTG
oRG768	TrueSeq Adapter (P7), Index 18	rev	CAAGCAGAAGACGGCATACGAGATgcggacGTGACTGGAGTTCAGACGTGTG
oRG769	TrueSeq Adapter (P7), Index 19	rev	CAAGCAGAAGACGGCATACGAGATtttcacGTGACTGGAGTTCAGACGTGTG